A method of estimating bulk potential permeability in fractured-rock aquifers using field-derived fracture data and type curves

Alex K. Manda · Stephen B. Mabee · David F. Boutt · Michele L. Cooke

Abstract A method is devised for estimating the potential permeability of fracture networks from attributes of fractures observed in outcrop. The technique, which is intended as a complement to traditional approaches, is based on type curves that represent various combinations of fracture lengths, fracture orientations and proportions (i.e., intensities) of fractures that participate in flow. Numerical models are used to derive the type curves. To account for variations in fracture aperture, a permeability ratio (R) defined as the permeability of a fracture network in a domain divided by the permeability of a single fracture with identical fracture apertures, is used as a dependent variable to derive the type curves. The technique works by determining the point on the type curve that represents the fracture characteristics collected in the field. To test the performance of the technique, permeabilities that were derived from fractured-rock aquifers of eastern Massachusetts (USA) are compared to permeabilities predicted by the technique. Results indicate that permeabilities estimated from type curves are within an order of magnitude of permeabilities derived from field tests. First-order estimates of fracture-network permeability can, therefore, be easily and quickly acquired with this technique before more robust and expensive methods are utilized in the field.

Keywords Modeling · Permeability · Fractured rocks · Type curves · USA

A. K. Manda (✉)
Department of Geological Sciences and Institute for Coastal Science and Policy,
East Carolina University,
387 Flanagan Building, East 5th Street, Greenville, NC 27858, USA
e-mail: mandaa@ecu.edu
Tel.: +1-252-3289403
Fax: +1-252-3284391

S. B. Mabee
Massachusetts Geological Survey,
University of Massachusetts Amherst,
611 N. Pleasant St., 233 Morrill Science Center, Amherst, MA 01002, USA

D. F. Boutt · M. L. Cooke
Department of Geosciences,
University of Massachusetts Amherst,
611 N. Pleasant St., 233 Morrill Science Center, Amherst, MA 01002, USA

Introduction

Fractures are common features in groundwater, geothermal and petroleum reservoirs where they play an important role in controlling the flow and storage of fluids in the subsurface (National Research Council 1996). The hydraulic properties of fractured media are thus controlled to a large extent by the apertures, trace lengths, spacings, orientations and connectivity of fractures (Robinson 1983; Berkowitz 1995; Zhang and Sanderson 1995; Odling 1997; de Dreuzy et al. 2001a). Owing to the important role that fractures play in channeling flow, the influence of fracture characteristics on the hydraulic properties of fractured bedrock aquifers has been the focus of research for decades. Long et al. (1982) used numerical models to assess conditions under which fractured media behave as equivalent porous media by varying fracture characteristics in two-dimensional (2D) models. They found that a network of fractures can be treated as a continuum when the density of fractures is high, the orientation distribution of fractures is non-uniform, apertures are constant and evaluated sample sizes are large relative to fracture sizes. In a later study, Long and Witherspoon (1985) were able to predict the permeability of fracture networks from orientation and intensity data derived from boreholes. However, their 2D numerical modeling experiments suggested that this was contingent upon the fracture length being above a critical size.

In recent times, other sophisticated approaches have been used to assess the effect of fracture attributes on the hydraulic properties of fracture networks (e.g., Huseby et al. 1997; Koudina et al. 1998). These numerical modeling procedures have advanced our understanding of the hydraulic properties of fracture networks by utilizing fractures with apertures that are correlated and

uncorrelated to fracture length (e.g., Mourzenko et al. 2004; Khamforoush et al. 2008). However, most of the numerical models used in these studies were not necessarily conditioned to field derived data (i.e., fracture attributes and hydrologic data).

Several researchers have attempted to condition their numerical models to field data (e.g., Caine and Tomusiak 2003; Min et al. 2004; Baghbanan and Jing 2007; Surrette et al. 2008; Surrette and Allen 2008). These researchers have employed correlated and uncorrelated fracture aperture and length data and/or used hybrid, discrete fracture network-equivalent porous medium (DFN-EPM) models to evaluate flow properties of fractured rocks. The results from these approaches have provided useful insights about the relation between fracture attributes and flow characteristics in fractured rocks. Despite these efforts, one still needs to utilize numerical models that require high technical expertise and specialized skills to estimate the permeability of fracture networks with known fracture attributes.

In this paper, a technique that utilizes fracture attributes collected from outcrop to quickly estimate the permeability of fractured rock aquifers without having to necessarily run complex numerical models is developed. Such a technique would be a valuable tool for field practitioners who may not have the time or skill to simulate groundwater flow in fracture networks. The approach presented here is based on the rationale that fracture attributes observed in outcrop can be used to estimate the hydraulic properties of fracture networks (Berkowitz 2002). The technique employs type curves of permeability ratios representing fracture networks with known fracture characteristics to estimate the potential permeability of fracture networks observed in the field. Using type curves would be complementary to traditional techniques for deriving permeabilities such as conducting aquifer tests, which may be laborious and/or expensive to perform.

There are five major components to this paper. The first part (section Attributes of natural fractures and development of synthetic fracture networks) consists of using fracture attributes collected from outcrops in the Nashoba terrane (eastern Massachusetts, USA; Fig. 1) in previous investigations (Manda et al. 2008) to derive acceptable ranges of attributes of real fractures. These ranges are then used to develop synthetic fracture networks that represent various combinations of fracture attributes. In the second part, the mechanism for estimating fracture network permeability using fracture attributes is developed by deriving equations that link the permeability of fracture networks to attributes of fractures—see section Permeability and permeability ratio (R). The next section (section Generation of type curves) — focuses on the generation of type curves using numerical modeling procedures. This section describes how the potential permeabilities of discrete fracture networks are
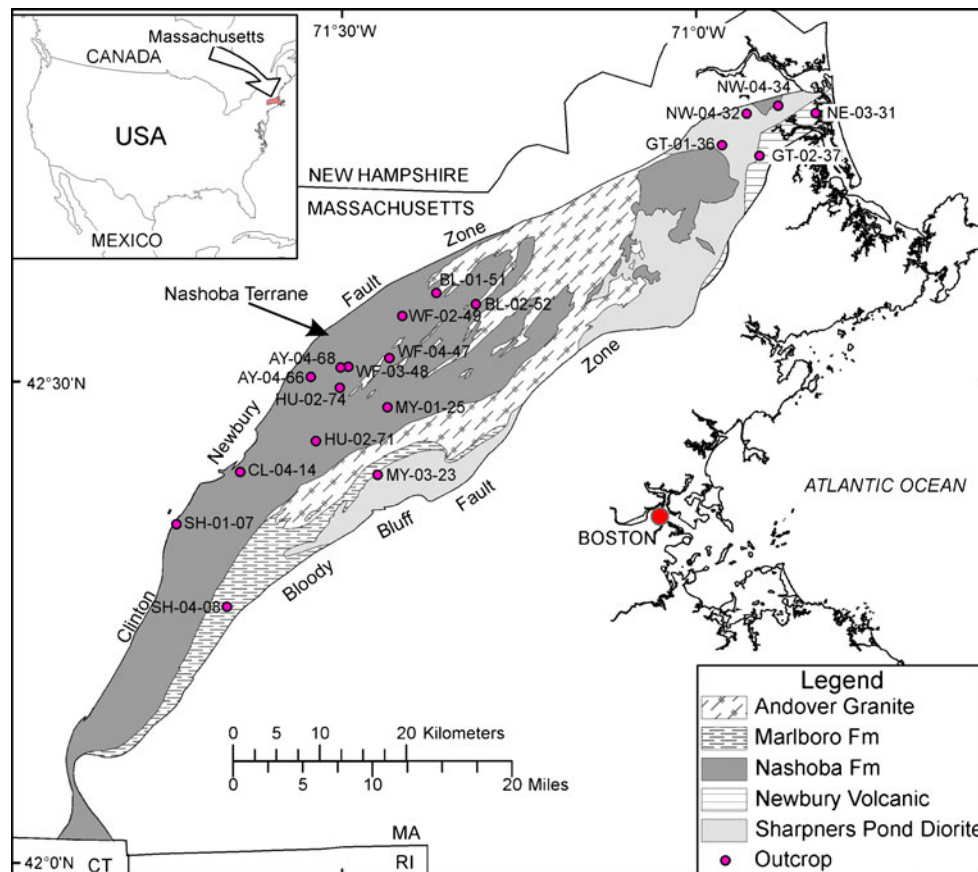

Fig. 1 Map showing distribution of outcrops where fracture data were collected in the Nashoba terrane, eastern Massachusetts, USA (base map modified from Zen et al. 1983)

estimated by simulating groundwater flow in multiple realizations of synthetic fracture networks. These estimates are used to compute permeability ratios from which type-curves are created. The following section (section Application) deals with testing the new technique against traditional methods by comparing the permeability derived from the type curves to the permeability acquired from pumping tests that were conducted in wells that are in close proximity to select outcrops. In the fifth part (section Discussion), the type curves are utilized to estimate the hydraulic properties of fracture networks from fractured aquifers in the Nashoba terrane with unknown permeabilities. Note that the type curves presented in this paper are not exhaustive, rather, these type curves serve as examples to highlight the potential benefits that the new technique can bring to field practitioners. Thus, the first three sections provide guidance to other researchers for creating additional type curves, whereas the last two sections provide a reference for using the current, though limited suite of type curves in the field.

Methodology

Attributes of natural fractures and development of synthetic fracture networks

In this section, fracture data collected from outcrops of the Nashoba terrane are used to define ranges of fracture attributes that are observed in natural fracture networks. This does not mean that the characteristics observed in outcrops of the Nashoba terrane are exhaustive of all the possible ranges of fracture attributes in nature. Rather, this approach is taken to make sure that the characteristics that are used to envision particular scenarios of fracture geometries and attributes are realistic and reasonable.

The majority of fractures measured by Manda et al. (2008) in the Nashoba terrane were measured on outcrops with long dimensions ≥5 m, suggesting that the lengths of sheeting joints are close to 5 m (Table 1). Tectonic joints and foliation parallel fractures in the terrane are shown to have mean trace lengths between 2 and 3 m, whereas mean fracture spacings are <1 m (i.e., intensities are >1 m^{-1}). The fracture data also reveal that some of the fracture networks that are observed in the terrane comprise sets with systematic fractures as evidenced by well-defined fracture sets (e.g., Fig. 2). Most of the fracture networks in the terrane comprise three fracture sets; there are two fracture sets that possess steep dips (sets I and III), whereas the other

fracture set (set II) has a moderate or shallow dip—refer to Figs. 1 and 5 in the electronic supplementary material (ESM) that accompany this paper.

Inspection of fracture data from the Nashoba terrane reveals that generally, two of the three fracture sets have nearly identical strikes (e.g., sets I and III in Fig. 2). However, the dihedral angles between these sets range from ~60 to 90° (Table 2). The dihedral angle is defined as the (acute) angle between two fracture planes as measured in a plane that is perpendicular to the first two planes (Marshak and Mitra 1988). The differences in strike between the two steepest fracture sets range from 70 to ~110° (Table 2). These observations suggest that the attributes of the fracture networks can be well represented by subdividing fracture sets into groups with various combinations of fracture lengths, intensities and relative orientations. Fracture sets can be represented by fractures with lengths of 2 and 5 m, intensities of 0.5, 1.0, 1.5 and 2.0 m^{-1}, dihedral angles of 60 and 80° for fracture sets with identical strikes, and a difference in strike of ~90° between the steepest fracture sets.

The fracture characteristics observed in nature are used to conceive multiple scenarios for building synthetic fracture networks comprising two- and three-fracture sets where at least two fracture sets have identical strikes. In the two-fracture set configuration, one fracture set is always vertical (set I), whereas the dip of the other set (set II) is set at 10° or 30° resulting in dihedral angles between sets I and II of 80° or 60° (Fig. 3a and b). In the three-fracture set configuration, the orientations of the first two sets are identical to those in the two-fracture set configuration, whereas the orientation of the third set (set III) is always vertical in each scenario. However, the third set maintains a trend difference of 90° with the other vertical set (i.e., the trends of sets I and III are perpendicular to each other) (Fig. 3c and d). The ranges used to devise these scenarios are chosen on the basis of the data and subdivisions described in the previous paragraph.

Since the trend of set III is always perpendicular to the other sets in each scenario representing the three-fracture set configuration, the dihedral angle is referenced between sets I and II in all cases. The dihedral angle, rather than the orientation of fracture sets (i.e., strike and dip), is the parameter which is preferred to capture the geometric arrangement of fractures in each network because the orientations of fracture sets in the field may not match the idealized orientations of fractures. The fracture sets in the field may have different orientations in space although the same sets may possess the same dihedral angles as the

Table 1 Statistics of fracture length and spacing derived from the Nashoba terrane for different fracture types. *FPF* foliation parallel fractures, *Min* minimum, *Max* maximum

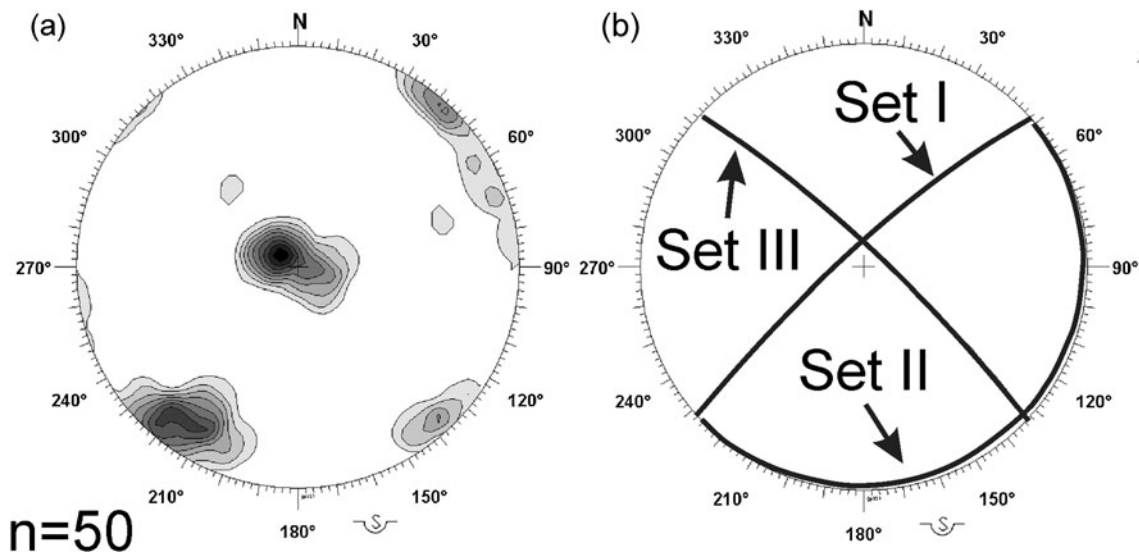| Fracture type	Fracture length (m)				Fracture spacing (m)			
	Mean	Min	Max	Count	Mean	Min	Max	Count
Tectonic joints	2.24	0.05	25	2,840	0.59	0.01	48	2,288
Sheeting joints	4.03	0.15	56	285	0.74	0.03	10	248
FPF	2.31	0.10	22	520	0.28	0.01	5	483
All fractures	2.39	0.05	56	3,645	0.55	0.01	48	3,019

Fig. 2 Examples of stereonets showing fracture data collected from an outcrop (WF0447) in the Nashoba Terrane. **a** Contoured equal area nets (contour interval=2 %) are used to identify fracture sets. **b** The mean orientations of the fracture sets are also plotted as great circles in stereonets

ones present in the idealized networks. The dihedral angle is therefore a better descriptor of the relative arrangement of fractures sets I and II than strike and dip.

Established discrete fracture network modeling techniques similar to those implemented by Caine and Tomusiak (2003) are used to simulate groundwater flow in three-dimensional (3D) numerical models of fracture networks. The commercially available FracMan software suite is used to build fracture networks in domains with various fracture attributes and configurations (Dershowitz et al. 1996). The volume of the model domain is based on a conservative estimate of the representative elementary volume that represents fracture networks with diverse fracture characteristics. Synthetic fractures in the fracture networks are generated in 10 m×10 m×10 m domains by

specifying in turn the intensities, orientations, lengths and length distributions of fracture sets. The rationale for using the 10 m×10 m×10 m model volume is given in Fig. 6 of the electronic supplementary material (ESM). Fracture orientation is modeled with no variability, whereas fracture lengths of 2 and 5 m have constant distributions. The reciprocal of fracture spacing is used to derive fracture intensities (Ortega et al. 2006). The Enhanced Baecher spacing model is used to generate fractures through a Poisson process from locations of fracture centers that are uniformly distributed within the model domain (Golder Associates 2004). Following the approach taken by Min et al. (2004), all fractures are initially modeled as polygons with constant apertures of 0.005 m even though fractures in nature have different attributes.

Table 2 Mean fracture orientations for fracture sets found at each outcrop in the Nashoba terrane. The dihedral angle (measured between fracture sets I and II) and the trend difference (measured between sets I and III) for each outcrop are also shown

| Site	Mean strike/dip			Dihedral angle (°)	Trend difference (°)	No. of fractures
	Set I	Set II	Set III			
AY0466	215/59	049/48	325/82	74	110	48
AY0468	217/85	102/08	143/77	71	74	15
BL0151	147/85	282/02	037/87	86	110	49
BL0252	309/76	216/09	056/82	77	73	22
CL0414	135/78	117/09	206/87	79	71	45
GT0136	222/89	080/10	123/86	79	99	57
GT0237	290/61	107/26	033/85	87	77	54
HU0271	139/75	088/29	231/81	59	92	16
HU0274	212/71	143/08	129/82	68	83	17
MY0125	163/77	047/08	056/82	81	107	26
MY0323	352/59	213/07	087/85	64	85	50
NE0331	069/62	233/61	139/81	59	70	43
NW0432	195/78	257/08	300/88	74	105	31
NW0434	053/82	078/13	145/88	70	92	34
SH0107	228/70	071/17	153/84	86	75	50
SH0408	043/90	199/13	307/84	88	84	63
WF0249	150/85	195/8	044/84	89	106	70
WF0348	340/89	077/12	047/89	90	113	61
WF0447	228/83	049/04	313/83	87	85	50
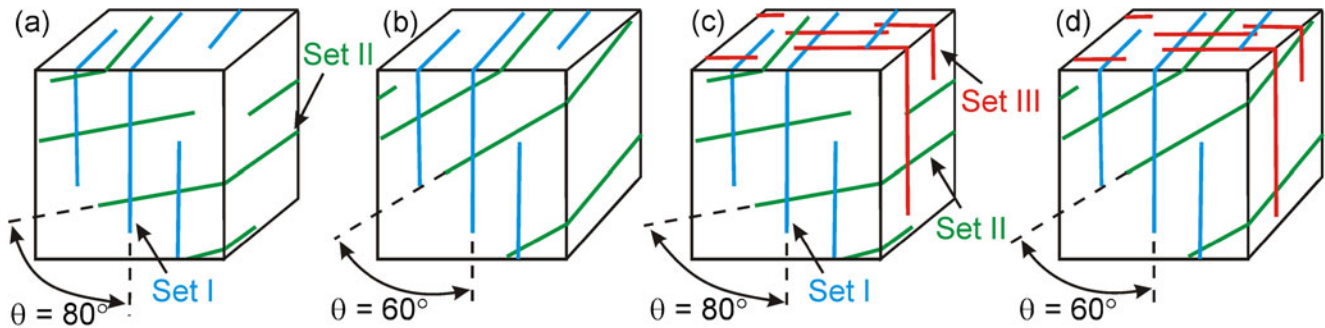
Fig. 3 Fracture configurations used to develop fracture networks. **a** Two-fracture set configuration where fracture sets *I* and *II* have identical strikes. Dihedral angle=*80°*. **b** Two-fracture set configuration where dihedral angle=*60°*. **c** Three-fracture set configuration where fracture sets I and II have identical strikes, and strike of set III is perpendicular to sets I and II. Dihedral angle=*80°*. **d** Three-fracture set configuration where dihedral angle=*60°*

Note that subsequent steps included a mechanism for deriving the permeability of a network that incorporates different fracture apertures (described in the following). An initial aperture of 0.005 m is used to simplify the modeling process, reduce the number of variables that are initially used, and to hasten the simulation procedure.

Since the synthetic fracture networks comprise two or three fracture sets, the length distributions for all sets are kept the same (i.e., all fracture sets in a given scenario are modeled with 2 or 5 m fracture lengths). Although the possible intensities of all hypothetical fracture sets range from 0.5 to 2 m^{-1} (in 0.5 m^{-1} intervals), the intensities of fracture sets I and III in the three-fracture-set networks are equal in every scenario. Making the intensity of set I equal to that of set III reduces the number of possible scenarios created. This approach reduces the number of potential results to a manageable size.

The following describes how various fracture networks are created with different permutations of fracture intensities (ranging from 0.5 to 2.0 m^{-1} for each fracture set). In the first scenario, fracture sets I and II (and set III for three-fracture-set networks) are each ascribed intensities of 0.5 m^{-1}. In the next permutations, the intensity of set II is then raised to 2.0 m^{-1} in increments of 0.5 m^{-1} while holding the intensity of set I (and set III) constant at 0.5 m^{-1}. The next round of scenarios involves ascribing an intensity of 1.0 m^{-1} to fracture set I (and set III) but an intensity of 0.5 m^{-1} to fracture set II. Then, while holding the intensity of fracture set I (and set III) constant (at 1.0 m^{-1}), the intensity of set II is increased from 0.5 to 2.0 m^{-1} in 0.5 m^{-1} increments. The process of increasing the intensity for each fracture set from 0.5 to 2.0 m^{-1} is repeated until all the possible permutations of the fracture intensities are generated. For a network with a specific fracture length and dihedral angle, a total of 12 scenarios are therefore conceived that capture all the combinations of the idealized fracture parameters. Once the fracture networks are generated, groundwater flow is then simulated in as many as 100 realizations that represent each of these scenarios.

Boundary conditions and flow simulation parameters that are assigned to the model domain are as follows. The domain is subjected to four no-flow boundaries and two specified head boundaries (Fig. 4). Flow is then simulated under steady-state conditions across the specified head boundaries of the model domain under a hydraulic gradient of 0.1. The boundary conditions are then switched to simulate flow across the other sides of the model domain. Using this approach, three permeability estimates are derived for each fracture network that is conceived by simulating flow in three mutually perpendicular directions, X, Y and Z (e.g., Caine and Tomusiak 2003; Surrette et al. 2008; Surrette and Allen 2008). A summary of the model parameters used is provided in Table 3. For each scenario conceived, 100 realizations are run in order to account for the variation in fracture location induced by the stochastic process of generating fractures.

Permeability and permeability ratio (R)
An important step in the development of the new technique involves the derivation of equations that link
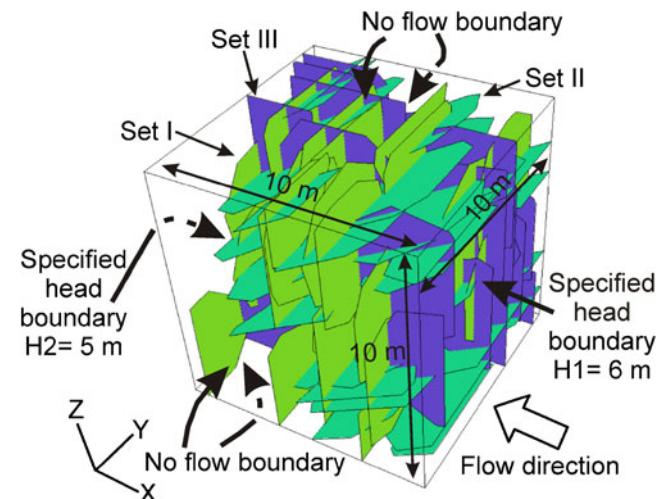

Fig. 4 Example of a model domain and boundary conditions used to simulate groundwater flow in discrete fracture networks. In this scenario, groundwater was simulated to flow in the *X* direction under a hydraulic gradient of 0.1. Flow in other directions was simulated by switching the boundary conditions of the model region. Note that the boundary conditions are applied across the faces of the cube

Table 3 Specifications used to develop synthetic fracture networks

Fracture specifications	Value/type
Domain size (m)	$10 \times 10 \times 10$
Model types	2 and 3 sets
Sets	Set I, set II, set III
Strike	090° (sets I and II) and 180° (set III)
Dip	90° (sets I and III) and 10°, 30° (set II)
Fracture geometry	8-sided polygon
Fracture length (m)	2 and 5
Size distribution	Constant
Spacing model	Enhanced Baecher
Set intensity (m^{-1})	0.5, 1.0, 1.5, 2.0
Initial aperture (m)	5×10^{-3}

the attributes of fractures to the permeability of fracture networks. To accomplish this, permeability is first computed from the median volumetric flow rate acquired by simulating flow in as many as 100 realizations for each scenario that is conceived. Darcy's Law is used to compute the equivalent bulk potential permeability of fracture networks for each of three mutually perpendicular flow directions to account for anisotropy:

$$k_{\mathrm{m}} = \frac{\mu Q_{\mathrm{m}}}{\rho g A I} \tag{1a}$$

where k_{m} = permeability of fracture network, Q_{m} = simulated volumetric flow through network with multiple fractures, A = specified cross sectional area across which flow occurs, μ = dynamic viscosity, ρ = density of water, g = acceleration due to gravity, and I = hydraulic gradient.

If the permeability of a single fracture in a domain is given by:

$$k_{\mathrm{f}} = \frac{\mu Q_{\mathrm{f}}}{\rho g A I} \tag{1b}$$

where k_{f} = permeability of single fracture in domain, and Q_{f} = simulated volumetric flow through a single fracture, then, the permeability of a fracture network can be normalized by the permeability of a single fracture giving:

$$R = \frac{k_{\mathrm{m}}}{k_{\mathrm{f}}} \tag{2}$$

where R = permeability ratio. R is constant provided all the fractures in both the fracture network and single fracture possess identical apertures. This relationship is only valid if: (1) the dimensions of the domains in which the fracture network and the single fracture are generated are identical (e.g., 10 m × 10 m × 10 m boxes), and (2) the single fracture has dimensions of 10 m × 1 m. Normalizing the permeability of the fracture network by the permeability of a single fracture ensures that multiple scenarios are represented by fewer results. Reducing the number of variables that are available serves to simplify the visualization of results.

If the cubic law (Snow 1968) is used to quantity the volumetric flow through a single fracture:

$$Q_{\mathrm{f}} = \frac{b^3 \rho g w I}{12\mu} \tag{3}$$

where b = fracture aperture and w = the width of the single fracture, then by combining Eqs. (1b) and (3), the permeability of the single fracture in the domain can also be expressed as:

$$k_{\mathrm{f}} = \frac{b^3 w}{12A} \tag{4}$$

Combining Eqs. (2) and (4) yields:

$$k_{\mathrm{m}} = \frac{b^3 w}{12A} R \tag{5}$$

In the current setup of fractures and model domains, $w = 1$ m, and $A = 100$ m^2, hence:

$$k_{\mathrm{m}} = \frac{b^3 R}{1200} \tag{6}$$

Equation (6) can therefore be used to estimate the permeability of a fracture network observed in outcrop if an estimate of the fracture aperture is known and an estimate of R is derived from a type curve. Detailed descriptions of how R is estimated from type curves are provided below.

Generation of type curves
Results of the numerical simulations described in the previous sections are used to create type curves representing R values of fracture networks with specific fracture attributes. Type curves are graphs where the fracture intensity for set II is plotted against R for networks with specific fracture lengths, and dihedral angles. The graphs have two lines of best fit which represent fracture networks with dihedral angles of 60 and 80°. To capture the intensities of fracture sets I and III, additional graphs are created that represent networks where the intensities of fracture sets I and III were ascribed in a predetermined manner (as described in section Attributes of natural fractures and development of synthetic fracture networks). A conceptualized representation of a suite of type curves for a 3-fracture-set network with a specified fracture length is shown in Fig. 5. Since there are multiple scenarios that represent fracture networks with different combinations of dihedral angles, fracture intensities and flow directions (for fracture networks with a specific fracture length), multiple graphs are required to capture the results from all these combinations—12 graphs in this case; see supplementary material Figs. 7–10 (ESM). As shown in Fig. 5, each row of graphs would represent the results from fracture networks with specified intensities of fracture sets I and III ranging from 0.5 to 2.0 m^{-1}, whereas
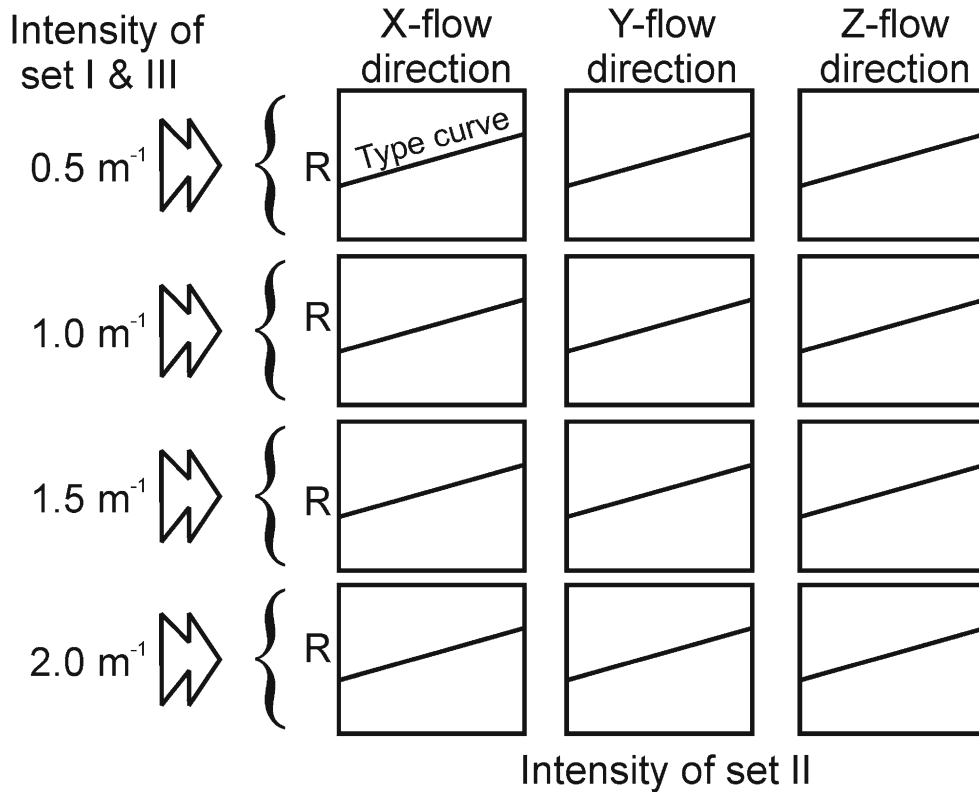
Fig. 5 Conceptual representation of type curves for a three-fracture set network with a specified fracture length. The graphs with the type curves are arranged in rows and columns. The *rows* represent fracture networks with predetermined intensities for fracture sets I and III, whereas the *columns* represent flow in each of three mutually perpendicular directions

the columns would represent the results from networks where flow was simulated in a specific direction (i.e., X, Y and Z). An estimate of *R* would then be derived by locating the point on the curve in the appropriate graph that represents the fracture network characteristics of interest.

Examples of type curves created from networks with 5 m trace lengths, and intensity of sets I and III=0.5 m^{-1} are shown in Fig. 6. Note that only one row of type curves is shown here for brevity—see Figs. 7–10 in ESM for complete suites of type curves representing two- and three-fracture-set networks comprising fractures with lengths of 2 and 5 m. The type curves show that all the fracture networks are anisotropic because the permeabilities are not equal in the X, Y and Z directions for fracture

networks with identical fracture attributes. Khamforoush et al. 2008 used analytical expressions that are based on the Snow (1969) model to relate the permeability of anisotropic fracture networks to the density of fracture networks. The Snow model relationships between density and permeability were shown to be linear for isotropic and anisotropic fracture networks. Thus, the trends of intensity of set II versus permeability ratio in this study are assumed to be linear. This assumption makes it easy to estimate permeability ratios using parameters for best-fit lines. As a consequence of the linear relationship between the intensity of set II and the permeability ratio, the type curve can be extrapolated to estimate the permeability ratio that corresponds to the intensity of set II that is larger than the predetermined range. A detailed description of
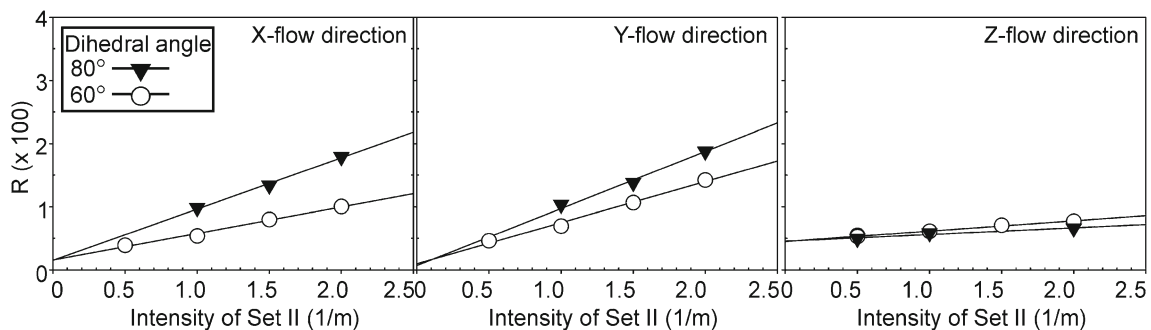

Fig. 6 Examples of type curves used to estimate the permeability ratio, *R*. Intensity of *set II* is plotted against *R*, which is derived by simulating flow in three mutually perpendicular flow directions *X*, *Y* and *Z*. The type curves shown are for fracture networks with dihedral angles of *80* and *60°*. Fracture lengths for all fracture sets are equal to 5 m, and intensities for fracture sets I and III are equal to 0.5 m^{-1}

how an estimate of permeability can be derived from information about fracture characteristics and type curves is given in the following section.

Application

To test the applicability of the new technique, permeabilities derived from type curves are compared to permeabilities derived from pumping tests that were performed in the Nashoba terrane by Boutt et al. (2010). First, fracture length, spacing and orientation data that were recorded from 19 outcrops located in the Nashoba terrane by Manda et al. (2008) are analyzed. Stereonets are used to delineate fracture sets and verify that the fractures in each set are systematic (e.g., Fig. 2). The mean orientation of each fracture set and dihedral angles between fracture sets I and II are computed (Table 2). The mean fracture lengths and estimates of intensity are then derived for each set (see Tables 1–3 in ESM). Fracture spacing is used to compute fracture intensity for all fracture sets.

In the Nashoba terrane, between 1 and 11 % of all the fractures that were logged in 17 bedrock wells are flowing (Diggins 2009). According to Boutt et al. (2010), flowing fractures are those fractures that contribute or remove water from a borehole. Thus, a conservative estimate of 10 % is used to quantify the proportion of fractures in each set that participate in flow in the terrane. This estimate is in agreement with estimates reported by other investigators who found that flowing fractures accounted for ≤10 % of fractures in their field areas (e.g., Shapiro and Hsieh 1991, 1994; Mazurek et al. 2003; Boutt et al. 2010). Since intensity values on the x-axis of the type curves are separated by discrete intervals, fracture intensities recorded from outcrops in the terrane are rounded up or down to match the values on the type curves (see Tables 1–3 in ESM). The consequence of this action is that the permeability estimated by the type curve may be under or over estimated.

The appropriate type curves need to be utilized to get the right estimate of R that corresponds to the fracture network with a specific set of fracture attributes. The procedure for estimating the permeability therefore consists of first selecting the graph representing a fracture network with the appropriate fracture lengths (for all fracture sets) and intensities (for sets I and III; Fig. 7). Then, the curve representing the appropriate dihedral angle is used to estimate R. This is achieved by locating the point on the curve that corresponds to the intensity of fracture set II. A horizontal line is extended from this point to the y-axis to read the value of R. This process is then repeated to estimate R in the other flow directions, before a geometric mean for R is calculated for all three flow directions.

Once R is estimated for a particular fracture network, Eq. (6) is used to estimate the permeability of the network by using an estimate of fracture aperture. An aperture-length correlation that is based on lognormal distributions
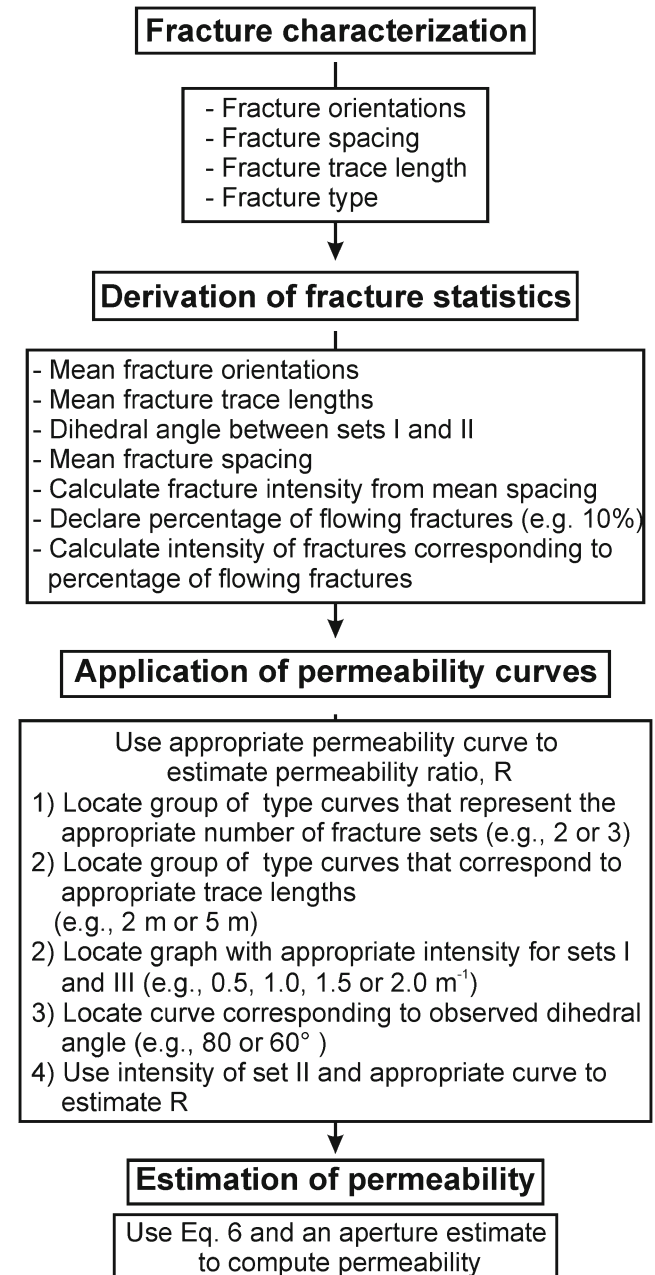
Fracture characterization
- Fracture orientations
- Fracture spacing
- Fracture trace length
- Fracture type

Derivation of fracture statistics
- Mean fracture orientations
- Mean fracture trace lengths
- Dihedral angle between sets I and II
- Mean fracture spacing
- Calculate fracture intensity from mean spacing
- Declare percentage of flowing fractures (e.g. 10%)
- Calculate intensity of fractures corresponding to percentage of flowing fractures

Application of permeability curves
Use appropriate permeability curve to estimate permeability ratio, R
1) Locate group of type curves that represent the appropriate number of fracture sets (e.g., 2 or 3)
2) Locate group of type curves that correspond to appropriate trace lengths (e.g., 2 m or 5 m)
2) Locate graph with appropriate intensity for sets I and III (e.g., 0.5, 1.0, 1.5 or 2.0 m^{-1})
3) Locate curve corresponding to observed dihedral angle (e.g., 80 or 60°)
4) Use intensity of set II and appropriate curve to estimate R

Estimation of permeability
Use Eq. 6 and an aperture estimate to compute permeability

Fig. 7 Flow chart of procedures used to estimate the permeability of fracture networks

of apertures (Baghbanan and Jing 2007) is used to derive estimates of fracture aperture. The apertures of fractures with 2 and 5 m lengths are found to be 9×10^{-5} m and 1.5×10^{-4} m, respectively, if a standard deviation of 1 assumed for the aperture distributions (Baghbanan and Jing 2007). Alternately, fracture apertures measured in the field may also be used in Eq. (6) to estimate the permeability. Since it is assumed that all the fractures in each model have fractures with identical lengths, the use of the single aperture measurement for all fractures is acceptable.

Of the 19 outcrops where appropriate fracture data were collected in the terrane, five are in close proximity to

wells where pumping tests were conducted to determine the permeability of fractured rock aquifers (Table 4). The close proximity of outcrops to wells facilitates the comparison of the permeability from wells to the permeability from outcrops where fracture attributes were acquired. Where possible, fracture data collected from the surface are compared to data derived from the subsurface (Manda et al. 2008; Diggins 2009; Boutt et al. 2010). This is done to confirm that fracture patterns observed on the surface extend into the subsurface.

Estimates of permeability derived from type curves of R are compared to corresponding permeabilities derived from field tests (Fig. 8). Results show that permeabilities derived from pumping tests are in agreement with those derived from type curves. Given that the type curves are created using parameters separated by predefined intervals, it is not always possible to match precisely the attributes derived from the field to those represented by the type curves. Therefore, ranges of fracture attributes that bracket field measurements are derived so that the permeabilities of fracture networks observed in the field can be approximated by the type curves. As a result of taking this approach, the permeabilities of fracture networks used in the test cases are reported as ranges of permeabilities for fracture networks with 2 and/or 5-m fracture lengths (Fig. 8). These permeability ranges also take into account the influence of multiple fracture intensities that can be approximated for each network with a specific fracture length (in addition to permeabilities derived from three flow directions). The geometric mean is then calculated for the range of permeability estimates representing the 2 and/or 5-m fracture lengths.

As an example, consider the fracture network at HU0271. The observed fracture lengths for fracture sets I, II and III are 0.7, 0.9 and 0.5 m, respectively, whereas the observed fracture intensities (for flowing fractures) for sets I, II and III are 0.36, 0.25 and 0.5 m^{-1}, respectively (see Tables 1–3 in ESM). However, the minimum length represented by the type curves is 2 m for all fracture sets, whereas the intensities for sets I, II and III are represented by 0.5, 0.25 and 0.5 m^{-1}, respectively. The dihedral angle computed for this fracture network is ~60°. To derive an appropriate R estimate for the network at HU0271, the observed fracture lengths and intensities are rounded up to match the values available on the type curve (see Fig. 8 in ESM). The fracture lengths for all fracture sets are
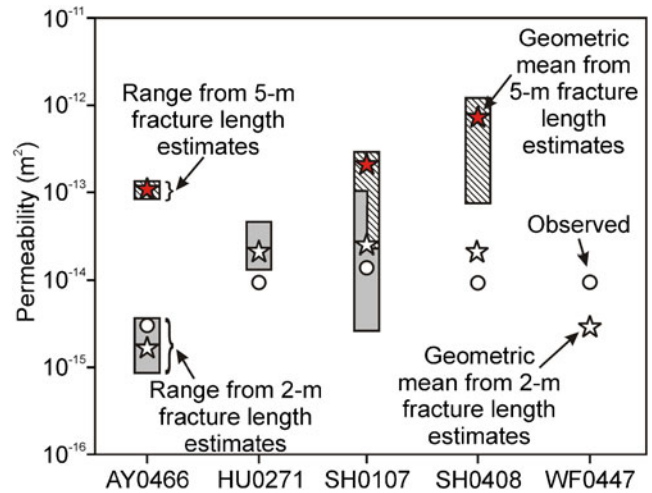

Fig. 8 Estimated ranges and observed values for permeability at select outcrops in the Nashoba terrane. The geometric means derived from fracture networks with fracture lengths of 2 m are within an order of magnitude of the observed permeabilities derived from field tests. *Open circles* = observed permeability, *open stars* = geometric mean of permeability from 2-m fracture networks, *filled/red stars* = geometric mean of permeability from 5-m fracture networks, *filled/grey rectangles* = range of permeabilities from fracture networks with 2 m fracture lengths, *hashed rectangles* = range of permeabilities from fracture networks with 5-m fracture lengths

rounded up to 2 m, whereas the intensity of fracture set I is rounded up to 0.5 m^{-1} (the intensity of fracture set III does not require rounding because it is already at 0.5 m^{-1}). The graph in the first row and first column of Fig. 8 in ESM (where the intensities of sets I and III=0.5 m^{-1}) is then used to estimate R. This is done by locating the point on the curve representing a dihedral angle of 60° and corresponding to an intensity of set II of 0.25 m^{-1}. A horizontal line drawn from this point to the y-axis provides an estimate of R in the X-flow direction (R_x=2.9) (see Table 4 in ESM). Similarly, estimates of R are derived from the graphs representing the Y- and Z-flow directions (R_y=2.0 and R_z=7.5). An estimate of fracture aperture is then used in Eq. (6) to estimate the permeabilities corresponding to the R values (see Table 4 in ESM). The computed permeabilities are thereafter used to define the range encompassing the permeability estimates from the fracture network at HU0271 (with 2-m fracture lengths; Fig. 8). The geometric mean computed from this range of permeability

Table 4 Attributes of wells, fracture networks and outcrops at select locations in the Nashoba terrane

Well[a]	Nearest outcrop[b]	Rock type	Fracture types[c]	% flowing[d]	Hydraulic conductivity, K (m/s)	Permeability, k (m^2)
Act1	WF0447	Mica schist	SJ, FPF	8	1.02E-07	1.04E-14
Shr1	SH0107	Amphibolite	SJ, TJ, FPF	4	1.43E-07	1.46E-14
Gates1	HU0271	Schist	SJ, TJ, FPF	2	8.93E-08	9.11E-15
Box1	AY0466	Mica schist	SJ, TJ, FPF	1	2.98E-08	3.04E-15
Sut1	SH0408	Amphibolite	SJ, TJ, FPF	10	9.23E-08	9.42E-15

[a] Well ID from Boutt et al. (2010)

[b] Outcrop ID from Manda (2009)

[c] Fracture types: *SJ* sheeting joints, *TJ* tectonic joints, *FPF* foliation parallel fractures

[d] *% flowing* percentage of fractures that were flowing

estimates is within an order of magnitude of the observed permeability.

When the geometric means for the rest of the test cases (AY0466, SH0107, SH0408 and WF0447) are compared to the observed permeabilities, the results reveal that the permeability estimates corresponding to the fracture networks with 2-m fracture lengths are within an order of magnitude of the observed permeability (Fig. 8). This is because the observed fracture lengths for fracture networks in the terrane are closer to 2 m than 5 m (see Tables 1–3 in ESM). These observations suggest that the technique performs reasonably well in estimating permeabilities of fracture networks that are observed in the field.

Discussion

Once the technique was verified, it was used to assess the variation of fracture network permeability in the Nashoba terrane using fracture attributes that were collected from the other 15 outcrops (see Table 5 in ESM). Because fracture attributes are rounded up or down to conform to the divisions used in the type curves, some outcrops have more than one estimate of potential permeability. These estimates are used to define permeability ranges from which the geometric means of the permeabilities of fracture networks are computed (as described in the previous section). The geometric means of the permeabilities representing the fracture networks are plotted on a basemap of the Nashoba terrane to assess the spatial variation of permeability in the region (Fig. 9). Only the permeability estimates from fracture networks with 2-m fracture lengths are shown on the Nashoba terrane basemap rather than the permeability estimates with 5-m fracture lengths because most of the observed fracture lengths in the terrane are close to 2 m (see Tables 1–3 in ESM).

The permeability map reveals that most of the sites with low permeability estimates (i.e., $<5.0 \times 10^{-15} \, \text{m}^2$) are located in the Nashoba formation (Fig. 9) where the dominant rock types are schists, gneisses and amphibolites. These rocks are dominated by foliation parallel fractures that trend in sympathy with the axial line of the Nashoba terrane (Manda et al. 2008). The data suggest that the change in orientation of the foliation parallel fractures does not significantly affect the permeability of the fracture networks in the Nashoba formation. The permeabilities of fracture networks in the northern parts of the Nashoba formation are similar to the permeabilities in the southern parts regardless of fracture trend. However, fracture networks with exceedingly high permeabilities (i.e., $> 15 \times 10^{-15} \, \text{m}^2$) are observed at SH0107 and AY0468. The fracture network located at SH0107 is in close proximity to the Clinton-Newbury fault zone. This could perhaps account for why this site has the highest permeability in the Nashoba formation.

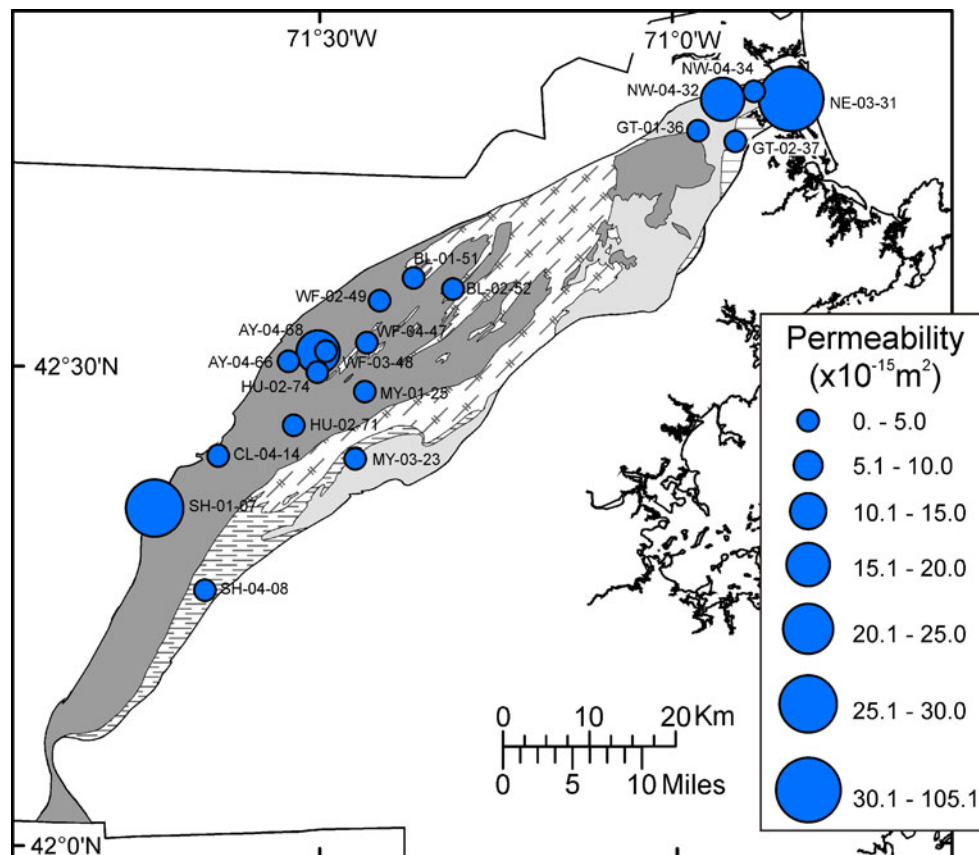There are several sites located in the Newbury volcanic complex, Marlboro, Sharpners Pond Diorite and Andover

Fig. 9 Estimates of permeability at outcrops with fracture sets that consist of systematic fractures in the Nashoba terrane. Note that the permeability is in units of $\times 10^{-15} \, \text{m}^2$. See Fig. 1 for legend of shading

Granite formations with fracture networks with varying permeabilities (Fig. 9). The fracture network located in the Newbury volcanic complex (NE0331) has the highest permeability (105×10^{-15} m^2) of all fracture networks in the Nashoba terrane. Fracture networks in the other formations have permeabilities that are no higher than 15×10^{-15} m^2. Unlike the fracture networks in the Nashoba formation, the networks in the Newbury volcanic complex, Marlboro, Sharpners Pond Diorite and Andover Granite formations are not influenced by the presence of foliation parallel fractures. Rather, these fracture networks are influenced by tectonic and sheeting joints. The interplay of various fracture attributes leads to differences in permeabilities of fracture networks that can be evaluated across the terrane.

Since the permeabilities of two or more fracture networks located in different terranes (or rock units) but having the same fracture network characteristics are expected to be identical, the type curves have universal application. Additionally, the type curves may be useful for assessing the permeabilities of fracture networks that are observed at the local scale without the need to conduct expensive pumping tests and time consuming numerical modeling experiments. The permeability estimates that are derived from outcrop data can then be used to indicate regions where potentially high-yielding water wells can be drilled. For example, the regions close to SH0107 and NE0331 appear to be favorable sites for drilling wells that would encounter fracture networks with relatively high permeability. Although lineaments identified on aerial photographs or satellite imagery are widely utilized to identify regions that may provide high-yield water wells in fractured bedrock terranes (e.g. Lattman and Parizek 1964; Siddiqui and Parizek 1971, 1974; Mabee et al. 1994), these techniques may not be adequate to identify sites for potentially high-yielding wells where lineaments are not easily identified (e.g., in the Nashoba terrane). The technique described here could therefore be used in regions where lineaments are not observed, but where fracture attributes can be derived from outcrop.

Limitations

There are several limitations that are inherent in the method used to estimate the permeability of fracture networks from type curves. First, parameters such as fracture roughness and effect of stress on fractures are not considered. This is done to simplify the procedure for estimating potential permeability. The type curves are constructed from data derived from simulating flow in fracture networks that comprise fracture sets with systematic fractures. Thus, the method shown here cannot be applied to fracture networks with randomly oriented fractures. Furthermore, only fracture networks with the appropriate number and configuration of fracture sets can be used for estimation. The networks should have at least two fracture sets where the first two sets possess identical strikes, whereas the strike of the third set is orthogonal to that of the first two sets. The proportion of fractures that are

hydraulically active is assumed to be 10 % for all fracture sets. However, individual fracture sets in the field may have different proportions of fractures that participate in flow. Thus, using the 10 % threshold for every fracture network may lead to under or over-estimation of fracture network permeability. If data are available from heat-pulse-flow-meter measurements, a representative measure of the proportion of fractures that participate in flow may be used to derive better estimates of the permeability of fracture networks.

Previous studies of fracture attributes in different rock types have revealed that fracture length may follow power-law and lognormal distributions (e.g., Wong et al. 1989; Odling 1997; Renshaw 1999; de Dreuzy et al. 2001b). Here, constant fracture length distributions, and length-aperture correlations are assumed for all fracture networks. Thus, the influence of fracture length variations may not be fully captured in the results. The type curves developed in this study are limited to fracture networks with fracture lengths of 2 or 5 m, fracture intensities of sets I and III that range from 0.5 to 2 m^{-1}, and dihedral angles between sets I and II of 60 and 80°. Because not all possible combinations of fracture attributes are represented by the type curves, it may not be possible to derive estimates of permeabilities for fracture networks with attributes that do not match the subdivisions listed in the preceding. Recall that these subdivisions are only derived from the Nashoba terrane; thus, additional subdivisions that may represent fracture networks in other terranes, regions or rock types may also be possible. Although the subdivisions that are used here do not represent all possible scenarios in nature, the ranges of lengths, intensities and dihedral angles that are utilized overlap those reported by researchers working in other regions (e.g., Hancock and Engelder 1989; Gillespie et al. 2001). An initial investment of time and resources is therefore required to derive additional type curves that represent assorted scenarios. However, once generated, these type curves would be available for application in diverse terranes without any need to run other simulations unless more detailed analyses are required. Thus, the type curves can be used to estimate the permeability of fractured rocks that possess negligible matrix permeability in regions other than the crystalline Nashoba terrane.

The technique presented here suffers from several limitations due to the simplifying assumptions made during the modeling process. However, these simplifications are necessary first steps for establishing a framework that uses numerical modeling results to create type curves. It is envisioned that as more type curves are developed and computing capabilities increase, the limitations associated with the technique will decrease.

Conclusions

Applied groundwater practitioners, modellers and researchers working in fractured rock terranes are usually interested in deriving a first-order estimate of the permeability of fractured rock aquifers. However, a simple technique for

estimating the permeability of fracture networks is not currently available. This paper presents a technique for estimating the permeabilities of fracture networks with fracture sets that comprises systematic fractures using type curves. The type curves rely solely on fracture characteristics observed in outcrop to derive an estimate of permeability.

The technique is tested by comparing the permeability estimated from fracture attributes using type curves to field data derived from pumping tests that were performed in the same rock units. Results from type curves are in agreement with the pumping test data to within an order of magnitude. The permeabilities of fracture networks at other sites within the terrane are then predicted to assess fracture network heterogeneity. The spatial distribution of permeability in the terrane suggests that the permeability in the Nashoba formation is uniform except for two locations where the proximity to an inter-terrane fault may influence hydraulic behavior. Permeabilities in other formations are generally comparable to those observed in the Nashoba formation with the exception that the highest permeabilities are observed in the Newbury Volcanic complex.

The technique developed here can be used as a complement to pumping tests and numerical modeling approaches for estimating permeability of fracture networks because it is inexpensive and easier to apply than traditional techniques. This technique is recommended as a first-order tool for assessing variation in fracture-network permeabilities but is certainly not intended to replace the need for site-specific aquifer tests and numerical modeling when the situation warrants more detailed work. Since there are an infinite number of combinations of fracture attributes, not all fracture attributes observed in the field are accounted for in the curves presented in this paper. It is therefore hoped that in the future, the range of combinations for fracture length, intensity and orientation that form the basis for type curves will be expanded to account for a variety of fracture attributes and permeabilities observed in the field.

References

Baghbanan A, Jing L (2007) Hydraulic properties of fractured rock masses with correlated fracture length and aperture. Int J Rock Mech Min Sci 44(5):704–719

Berkowitz B (1995) Analysis of fracture network connectivity using percolation theory. Math Geol 27(4):467–483

Berkowitz B (2002) Characterizing flow and transport in fractured geologic media: a review. Adv Water Resour 25:861–884

Boutt DF, Diggins PJ, Mabee SB (2010) A field study (Massachusetts, USA) of the factors controlling the depth of groundwater flow systems in crystalline fractured-rock terrain. Hydrogeol J 18(8):1839–1854. doi:10.1007/s10040-010-0640-y

Caine JS, Tomusiak SRA (2003) Brittle structures and their role in controlling porosity and permeability in a complex Precambrian crystalline-rock aquifer system in the Colorado Rocky Mountain Front Range. Geol Soc Am Bull 115(11):1410–1424

de Dreuzy JR, Davy P, Bour O (2001a) Hydraulic properties of two-dimensional random fracture networks following a power law length distribution, 1: effective connectivity. Water Resour Res 37(8):2065–2078

de Dreuzy JR, Davy P, Bour O (2001b) Hydraulic properties of two-dimensional random fracture networks following a power law length distribution, 2: permeability of networks based on lognormal distribution of apertures. Water Resour Res 37(8):2079–2095

Dershowitz W, Lee G, Geier J, Foxford T, LaPointe P, Thomas A (1996) FracMan™: interactive discrete feature data analysis, geometric modeling, and exploration simulation, user documentation, version 2.5. Golder, Redmond, WA

Diggins JP (2009) Understanding the Depth and Nature of Flow Systems in the Nashoba Terrane, Eastern Massachusetts, U.S.A. MSc Thesis, University of Massachusetts, USA. http://scholarworks.umass.edu/theses/272. Accessed January 2012

Gillespie PA, Walsh JJ, Watterson J, Bonson CG, Manzocchi T (2001) Scaling relationships of joints and vein arrays from The Burren Co. Clare, Ireland. J Struct Geol 23:183–201

Golder Associates (2004) FracWorks XP: discrete feature simulator, User Documentation, Version 4.0. Golder, Redmond, WA

Hancock PL, Engelder T (1989) Neotectonic joints. Geol Soc Am Bull 101:1197–1208

Huseby O, Thovert J-F, Adler PM (1997) Geometry and topology of fracture systems. J Phys A Math Gen 30:1415–1444

Khamforoush M, Shams K, Thovert J-F, Adler PM (2008) Permeability and percolation of anisotropic three-dimensional fracture networks. Phys Rev 77(5):0563071–056307110

Koudina NR, Garcia G, Thovert J-F, Adler PM (1998) Permeability of three-dimensional fracture networks. Phys Rev 57(4):4466–4467

Lattman LH, Parizek RR (1964) Relationship between fracture traces and the occurrence of groundwater in carbonate rocks. J Hydrol 2:73–91

Long JCS, Witherspoon PA (1985) The relationship of the degree of interconnection to permeability in fracture networks. J Geophys Res 90:3087–3098

Long JCS, Remer JS, Wilson CR, Witherspoon PA (1982) Porous media equivalents for networks of discontinuous fractures. Water Resour Res 18(3):645–658

Mabee SB, Hardcastle KC, Wise DU (1994) A method for collecting and analyzing lineaments for regional-scale fractured bedrock aquifer studies. Ground Water 32(6):884–894

Manda AK (2009) Development and verification of conceptual models to characterize the fractured bedrock aquifer of the Nashoba terrane, Massachusetts. PhD, University of Massachusetts, USA, paper AAI3372266. http://scholarworks.umass.edu/dissertations/AAI3372266. Accessed January 2012

Manda AK, Mabee SB, Wise DU (2008) Influence of rock fabric attribute distribution and implications for groundwater flow in the Nashoba Terrane, eastern Massachusetts. J Struct Geol 30(4):464–477

Marshak S, Mitra G (1988) Basic methods of structural geology. Prentice Hall, Upper Saddle River, NJ

Mazurek M, Jakob A, Bossart P (2003) Solute transport in crystalline rocks at Äspö: geological basis and model calibration. J Contam Hydrol 61:157–174

Min KB, Jing L, Stephansson O (2004) Determining the equivalent permeability tensor for fractured rock masses using a stochastic

REV approach: method and application to the field data from Sellafield, UK. Hydrogeol J 12:497–510

Mourzenko VV, Thovert J-F, Adler PM (2004) Macroscopic permeability of three-dimensional fracture networks with a power-law size distribution. Phys Rev 69(6):0663071–06630713

National Research Council (1996) Rock fracture and fluid flow, contemporary understandings and applications. National Academy Press, Washington, DC

Odling NE (1997) Scaling and connectivity of joint systems in sandstones from western Norway. J Struct Geol 19:1257–1271

Ortega O, Marrett R, Laubach S (2006) A scale-independent approach to fracture intensity and average spacing measurement. AAPG Bull 90(2):193–208. doi:10.1306/08250505059

Renshaw CE (1999) Connectivity of joint networks with power law length distributions. Water Resour Res 35:2661–2670

Robinson PC (1983) Connectivity of fracture systems a percolation theory approach. J Phys A Math Gen 16:605–614

Shapiro A, Hsieh P (1991) Research in fractured-rock hydrogeology: characterizing fluid movement and chemical transport in fractured rock at the mirror lake drainage basin, New Hampshire. In: US Geological Survey Toxic Substances Hydrology Program: Proc. of the technical meeting, Monterey, CA, March 11–15, 1991. US Geol Surv Water Resour Invest Rep 91–4034

Shapiro A, Hsieh P (1994) Hydraulic characteristics of fractured bedrock underlying the FSE well Field at the mirror lake site, Grafton County, New Hampshire. In: US Geological Survey Toxic Substance Hydrology Program: proceedings of the technical meeting, Colorado Springs, CO, September 20–24, 1993. US Geol Surv Water Resour Invest Rep 94–4015

Siddiqui SH, Parizek RR (1971) Hydrologic factors influencing well yields in folded and faulted carbonate rocks in central Pennsylvania. Water Resour Res 7(5):1295–1312

Siddiqui SH, Parizek RR (1974) An application of non parametric statistical tests in hydrogeology. Ground Water 12:1–14

Snow DT (1968) Rock fracture spacings, openings, and porosities. Proc Am Soc Civ Eng J Soil Mech Found Div ASCE 94:73–91

Snow DT (1969) Anisotropic permeability of fractured media. Water Resour Res 5(6):1273–1289

Surrette MJ, Allen DM (2008) Quantifying heterogeneity in variably fractured sedimentary rock using a hydrostructural domain. Geol Soc Am Bull 120:225–237. doi:10.1130/B26078.1

Surrette MJ, Allen DM, Journey M (2008) Regional evaluation of hydrologic properties in variably fractured rock using a hydrostructural domain approach. Hydrogeol J 16:11–30. doi:10.1007/s10040-0070206-9

Wong TF, Fredrich JT, Gwanmesia GD (1989) Crack aperture statistics and pore space fractal geometry of westerly granite and Rutland quartzite: implications for an elastic contact model of rock compressibility. J Geophys Res 94 (B8):10,278. doi:10.1029/JB094iB08p10267

Zen E, Goldsmith RR, Ratcliff NM, Robinson P, Stanley RS (1983) Bedrock geologic map of Massachusetts. U S Geol Surv scale 1:250000

Zhang X, Sanderson DJ (1995) Anisotropic features of geometry and permeability in fractured rock masses. Eng Geol 40:65–75